Modeling Reconfigurable Intelligent Surfaces-aided Directional Communications for Multicast Services

Olga Chukhno*,‡, Nadezhda Chukhno*,†, Sara Pizzi*, Antonella Molinaro*,§, Antonio Iera¶, Giuseppe Araniti*
*University Mediterranea of Reggio Calabria, Italy and CNIT, Italy
‡Tampere University, Finland
†Universitat Jaume I, Castelló de la Plana, Spain
§Université Paris-Saclay, Gif-sur-Yvette, France
¶University of Calabria, Italy and CNIT, Italy
e-mail: {*olga.chukhno, nadezda.chukhno, sara.pizzi, antonella.molinaro, araniti*}*@unirc.it*, *antonio.iera@dimes.unical.it*

***Abstract*—According to the 6G vision, the evolution of wireless communication systems will soon lead to the possibility of supporting Tbps communications, as well as satisfying, individually or jointly, a plethora of other very stringent quality requirements related to latency, bitrate, and reliability. The achievement of these goals will naturally raise many research issues within radio communications. In this context, a promising 6G wireless communications enabler is the reconfigurable intelligent surface (RIS) hardware architecture, which has already been recognized as a game-changing way to turn any naturally passive wireless communication setting into an active one. This paper investigates RIS-aided multicast 6G communications by first modeling the system delay as a first-come-first-served (FCFS) M/D/1 queue and analyzing the behavior under different blockage conditions. Then the study of multi-beam operation scenarios, covering multicast and RIS-aided multicast communications, is conducted by leveraging an M/D/c queue model. Achieved results show that large-size RISs outperform even slightly obstructed direct BS-to-user paths. In contrast, RISs of smaller sizes require the design of sophisticated power control and sharing mechanisms to achieve better performance.**

***Index Terms*—6G, wireless communication, millimeter wave, multicast, reconfigurable intelligent surfaces, queuing theory.**

I. Introduction

Novel and high-demanding services have sparked recent research initiatives on new wireless hardware designs and connectivity concepts for 6G wireless communications to satisfy various energy efficiency, throughput, latency, and reliability requirements [1]. Wireless communications assisted by reconfigurable intelligent surface (RIS), also known as intelligent reflecting surface (IRS), are a prominent research topic in academia and industry and have already drawn much attention for future 6G wireless networks. RIS improves systems' spectrum usage and energy efficiency by artificially reconfiguring the propagation environment. Meanwhile, the utilization of the millimeter wave (mmWave) and submillimeter, or equally terahertz (THz) spectrum, provides several advantages together with many challenges. The penetration and *reflections* from various materials are the critical aspects that have to be taken into account in such extremely high frequency (EHF) bands. In this vein, RIS can improve the channel state, suppress interference, enhance system performance, and can be easily placed in different locations such as indoor walls, cars, buses, and building facades, among others.

Increased data rate demands have fostered the transition from 5G to 6G communication systems, with a focus also on broadcast/multicast transmissions. Multicast transmissions based on content reuse, in its turn, have already attracted a lot of research interest, thanks to their high potential to improve bandwidth efficiency in future wireless networks compared to unicast transmissions [2]. Multicast communications are commonly used in many application contexts, such as video gaming, television broadcasting, and video conferencing, among others. Practically, in multi-group multicast communications, each group receives identical content, and the data rate of each group is determined by the user equipment (UE) device with the weakest channel gain. A few research groups conducted some studies on RIS-assisted multicast systems to address the mentioned issue. For example, in [3], a RIS-assisted multicast architecture is proposed, whereas in [4], the channel conditions of the weakest UE are improved by carefully configuring the RIS phase shifts. A RIS-assisted multicast communication has been investigated in [5] to achieve the locally optimal phase shifts based on a capacity optimization problem. In [6], system-level simulations have been performed that have shown that the near-field region may not be ignored in outdoor scenarios.

However, there has been little effort on theoretical models for RIS-aided multicast 6G communications. Therefore, there is still a need for an analytical assessment of such systems to capture the effect of antenna, propagation, and blockage patterns. This work contributes to bridge this gap by leveraging queuing theory tools to model multicast wireless communications assisted by RIS. Specifically, we first provide a model of the delay in multicast 5G and in RIS-aided multicast 6G communications as a first-come-first-served (FCFS) M/D/1 queue. We then analyze the system under different blockage conditions. Finally, we examine multi-beam operation scenarios utilizing the M/Dc queue. The remainder of the paper is laid out as follows. The system model is detailed in Section II. Section III illustrates how the system delay and cumulative density function (CDF) of the system time are computed based on the M/D/1 and M/D/c queue models. Section IV contains

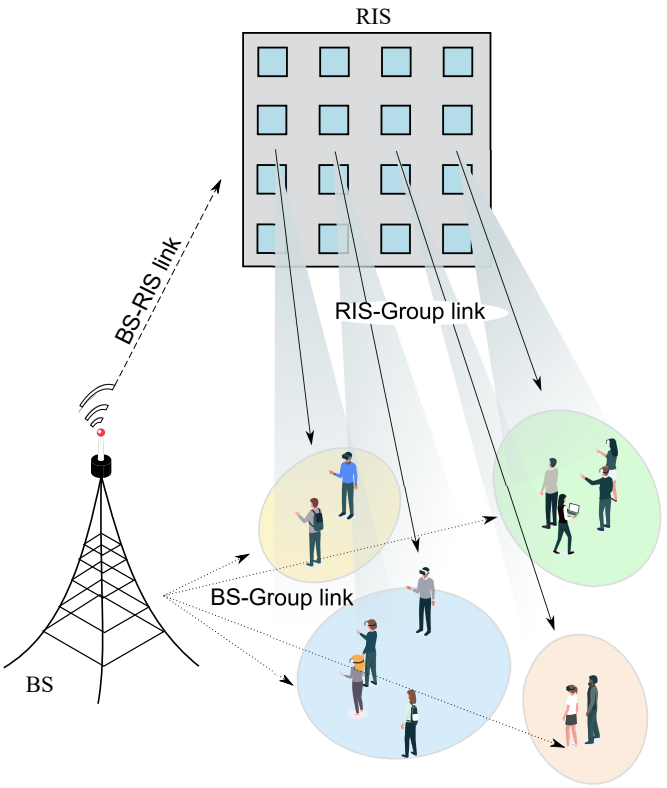

Fig. 1: RIS-aided multicast systems.

numerical results validated with the simulation campaign. Conclusions are drawn in Section V.

II. System Model

This section outlines the system model, including deployment, antenna, propagation, and blockage components.

A. Deployment

We consider a wireless communication system, shown in Fig. 1, with a single RIS, a single base station (BS), and multiple multicast groups, each including mobile user equipment (UE) devices of different nature. All UEs are equipped with mmWave modules and connected to the NR BS operating in the mmWave frequency band of 28 GHz. We assume the height of the NR BS to be constant and set to h_{BS}. NR BS has R_d coverage radius within which it is assumed that all UEs successfully receive data. A RIS is placed 14 m far away from the NR BS (the optimal placement for RIS [7]) and is assumed to be in the far-field with a LoS path to/from the RIS [8].

The locations of UEs, $\mathcal{N}_{\text{UE}} = \{1, ..., N_{\text{UE}}\}$, are assumed to be scattered around the plane according to an independent homogeneous point process with a predefined density λ_{UE}. The UEs move according to the Headed Social Force Model [9]. We also suppose that the mobile crowd can block UEs in our scenario of interest (see Section II-C).

B. Antenna and Propagation

We assume a conical antenna pattern, i.e., a unique beam shape in the elevation and azimuth planes. For this purpose, we approximate the beamforming pattern as proposed in [10]. Therefore, the transmit/receive antenna gains are given by

$$G_{\text{tx}} = D_0 \rho(\alpha), \tag{1}$$

where D_0 is the maximum directivity along the antenna boresight, α corresponds to the angular misalignment of the transmit/receive direction from the receiver's boresight, whereas $\rho(\alpha) \in [0; 1]$ is a piecewise linear function [10].

Following 3GPP, we adopt the 3GPP urban microcell (UMi) street canyon path loss model [11]:

$$L_{\text{dB}}(y) = 32.4 + 21 \log_{10} y + 20 \log_{10} f_c, \tag{2}$$

where y is the three-dimensional distance between the NR BS and a UE, whereas f_c is the operating frequency in GHz.

The total received power at distance y is calculated as

$$P_{\text{rx}} = P_{\text{tx}} G_{\text{tx}} G_{\text{rx}} L^{-1}(y) = \frac{P_{\text{tx}} G_{\text{tx}} G_{\text{rx}}}{L(y)}, \tag{3}$$

where $G_{\text{tx}} = D_0 \rho(\alpha)$ is the transmit antenna gain, G_{rx} is the receive antenna gain, $L(y)$ is the path loss in linear scale, i.e., $L(y) = A y^{\zeta}$ with

$$A = 10^{2 \log_{10} f_c + 3.24}, \ \zeta = 2.1, \tag{4}$$

where A and ζ correspond to the propagation coefficients.

For RIS, similarly, 3GPP UMi street canyon path loss models are utilized to express the path loss of sub-paths, which are defined from an NR BS to a RIS, $L(y_{\text{BR}})$, and from a RIS to a UE, $L(y_{\text{RU}})$. The total received power at the UE through the RIS element i is calculated as [12]:

$$P_{\text{rx},i} = \frac{P_{\text{tx}} |\Gamma_i| G_{\text{tx}} G_{\text{rx}}}{L(y_{\text{BR}}) L(y_{\text{RU}})}, \tag{5}$$

where Γ_i is the reflection coefficient of the ith RIS element, which is given by

$$\Gamma_i = e^{-j\varphi_i} G_i^e G_r^e \epsilon_b, \tag{6}$$

where φ_i is the phase difference inducted by RIS element i, G_i^e is the gain of the RIS in the direction of incoming wave, G_r^e is the gain of the RIS in the direction of received wave, and ϵ_b is the efficiency of RIS, which is described as the ratio of the power of the signal transmitted by the RIS to the power of the signal received by the RIS. In this paper, we assume $\epsilon_b = 1$ [7].

The total received power at the receiver, including all RIS elements, is expressed as:

$$P_{\text{rx}} = \left(\sum_i \sqrt{\frac{P_{\text{tx}} |\Gamma_i| G_{\text{tx}} G_{\text{rx}}}{L(y_{\text{BR}}) L(y_{\text{RU}})}} e^{j\phi_i} \right)^2, \tag{7}$$

where ϕ_i represents the phase delay of the signal received through the RIS element i.

For the sake of simplicity, we assume that RIS-elements reflect signal with unit-gain reflection coefficients ($|\Gamma_i| = 1$) and the signals coming through different RIS elements are aligned in phase at the receiver ($\phi_i = \varphi_i$) [7].

We highlight that, in our work, we employ a simple 3GPP formulation where the effect of small-scale fading is disregarded (only the mean path loss value is computed). For simplicity, and especially because we are targeting the mean capacity values, we do not consider small-scale fading. However, small-scale path loss and shadowing can be incorporated into our proposed framework.

We also assume that beamsteering is employed at all the communicating nodes, which minimizes the level of interlink interference, thus making the considered mmWave regime noise-limited [13]. Then, the per-antenna power budget is considered for the transmissions scheduled at the same time (as described in Section III-B). This means that the maximum transmission power has to be split among the beams that are active at the same time.

C. Blockage

Blockers are modeled as cylinders with a constant base radius and a constant height, r_B and h_B, respectively. The signal attenuation due to human blockage is assumed to be 15 dB [14]. The number of blockers follows a Poisson distribution with the density of λ_B per square meter. The blockage probability at the distance y is determined as in [15]:

$$p_B(y) = 1 - e^{-2\lambda_B r_B \left[\sqrt{y^2-(h_{BS}-h_{UE})^2}\frac{h_B-h_{UE}}{h_{BS}-h_{UE}}+r_B\right]}, \quad (8)$$

where h_{UE} is the UE height, $h_B \geq h_{UE}$.

In city deployments, a building blockage model is needed. According to the 3GPP UMi street canyon model [11], the LoS probability for the two-dimensional distance x between the NR BS and a UE, $p_L(x)$, is given by

$$p_L(x) = \begin{cases} 1, & x \leq 18\text{m}, \\ \frac{18}{x} + e^{-\frac{x}{36}}\left(1-\frac{18}{x}\right), & x > 18\text{m}. \end{cases} \quad (9)$$

Note that RIS serves as a means to avoid building blockage. Hence, we assume that building blockage affects only RIS-less multicasting.

III. M/D/1 and M/D/c models for Multicasting

In this work, we consider the downlink direction of transmissions. The transmission procedure of both multicast and RIS-aided multicast communications is modeled by means of M/D/1 and M/D/c queues for single- and multiple-beam antenna design systems, respectively (see Fig. 2). The service time is assumed to follow a deterministic distribution depending on the channel conditions of the UEs involved in multicast services.

A. M/D/1 for Single-Beam Multicasting

We first consider a single-beam antenna operation at the NR BS and model it as an M/D/1 queue. The M/D/1 queue is a stochastic process with packet arrivals generated by Poisson process rate λ and deterministic service time D with rate $\mu = 1/D$. According to the FCFS principle, data packets are processed one at a time based on their position in the queue. There is no limit to the number of packets stored in the buffer.

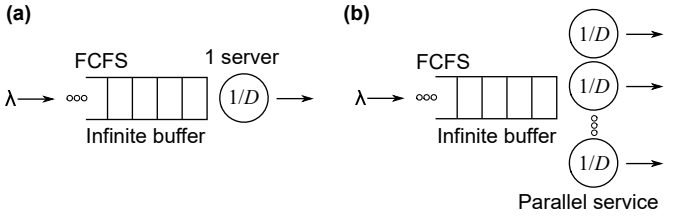

Fig. 2: Illustration of (a) M/D/1 and (b) M/D/c queuing nodes in Kendall's notation.

The waiting time cumulative distribution function (CDF) with arrival rate λ and deterministic service time D is as follows [16]:

$$P_W(w) = (1-\lambda D)\sum_{k=0}^{\frac{w}{D}} \frac{[\lambda(kD-w)]^k}{k!} e^{-\lambda(kD-w)}. \quad (10)$$

Proof. Erlang's derivation can be found in [16]. □

The waiting time probability density function (PDF) with arrival rate λ and deterministic service time D can be derived by differentiating (10) as follows:

$$p_W(w) = \frac{d}{dw}\left[(1-\lambda D)\sum_{k=0}^{\frac{w}{D}} \frac{[\lambda(kD-w)]^k}{k!} e^{-\lambda(kD-w)}\right]$$
$$= (1-\lambda D)\left[\lambda e^{\lambda w} + \sum_{k=1}^{\frac{w}{D}} \frac{\lambda^k [kD-w]^{k-1}}{k!} e^{-\lambda(kD-w)}(k-\lambda(kD-w))\right],$$
$$p_W(0) = 1-\lambda D, \quad (11)$$

where $w > 0$.

The average time in the system is given by:

$$W_S = \frac{2-\lambda D}{2\mu(1-\lambda D)}. \quad (12)$$

The average waiting time in the queue can be obtained as follows:

$$W_Q = \frac{\lambda D}{2\mu(1-\lambda D)}. \quad (13)$$

B. M/D/c for Multi-Beam Multicasting

We then characterize a multi-beam antenna operation system as the M/D/c queue. The M/D/c queue is a stochastic process with deterministic service time D, packet arrivals generated by the Poisson process rate λ, c identical servers, and buffer of infinite size. Along with the M/D/1 system, UEs' packets are processed according to the FCFS concept. In this work, we associate c with the number of concurrent beams at the NR BS.

The waiting time CDF with arrival rate λ and deterministic service time D for M/D/c is given by [16]

$$F(z) = \int_o^{\infty} F(w+z-D)\frac{\lambda^c w^{c-1}}{(c-1)!} e^{-\lambda w\, dw}, \quad (14)$$

where $z \geq 0$.

Then, CDF of the waiting time with arrival rate λ and deterministic service time D for M/D/c has been derived in closed form in [17] for $(k-1)D \leq w < kD$ as follows:

$$P_W(w) = \sum_{j=0}^{kc-1} Q_{kc-j-1} \frac{\lambda^j (kD-w)}{j!} e^{-\lambda(kD-w)}, \quad (15)$$

where $w = kD - u$, whereas u is the the positive time lapse, $0 < u \leq D$. The term Q_{kc-j-1} is expressed by

$$Q_{kc-j-1} \equiv \sum_{l=0}^{kc-1} q_l, \quad (16)$$

where q_l represents the stationary probability of finding queue of length l.

Proof. Franx's derivation can be found in [17]. □

C. Notes

For both M/D/1 and M/D/c queue-based systems, the service time corresponds to the deterministic time D with rate $\mu = 1/D$. Therefore, the CDF of the total time in the system can be derived as follows [18]:

$$P_T(t) = P_W(t-D)I(t-D), \quad (17)$$

where $I(.)$ represents the step function.

We note that the M/D/1 and M/D/c queues are suitable for modeling both multicast and RIS-aided multicast downlink transmissions with single- and multi-beam antenna operations, respectively. The difference in the modeling of multicasting and RIS-aided multicasting is in the deterministic value of service time, D. This value depends on the channel conditions, as described in Section II, namely on the received power as per (3) and (7), as well as other characteristics such as antenna/RIS models, number of antenna/reflective elements, and blockage conditions that are avoided when utilizing RIS. We recall that the data rate of the multicast session depends on the instantaneous channel of the worst UE in the multicast group.

IV. Selected Numerical Results

This section provides selected numerical results to evaluate the performance of 5G multicast and 6G RIS-aided multicast mmWave systems. We consider devices' operation via 5G NR BS at 28 GHz as a representative scenario. UEs are involved in multicast services such as collective XR or virtual games. The mobility simulation is built on a social force-based model [9]. By default, the UEs move at an average speed of 0.69 m/sec. The transmit power is fixed at the level of $P_{tx} = 46$ dBm. We utilize antenna array with 32×32, 16×16, 8×8, 4×4, and 2×2 antenna elements depending on the location of UEs' belonging to the multicast groups. RIS paths are assumed to be LoS but can be blocked by the moving crowd (see Section II-C). The remaining simulation parameters are reported in Table I.

We start by validating the proposed analytical framework in the case of a single-beam system, i.e., M/D/1 queue model. To verify our analytical queuing theory model, we compare the basic metrics, i.e., the average delay in the system and its CDF, against those obtained with Monte Carlo simulation in which 10^5 packets have been sent. For any given value on the x-axis, the CDF of the system time shows the percentage of UEs being in the system for a time equal to or below x value. As one may observe from Fig. 3, the simulation data are very close to theoretical results, which demonstrates the applicability of the M/D/1 queuing model to 5G multicast and 6G RIS-aided multicast systems. Therefore, we rely upon our developed analytical model. We also validate the M/D/c queuing model and analyze the multi-beam systems later in this section.

Generally, RIS is deployed to provide LoS non-blocked paths, thereby enhancing the system performance. In Fig. 3, we consider the scenario when RIS paths are never blocked, while in Fig. 4, we consider a worst-case scenario for RIS, i.e., RIS paths can be impeded. In particular, we investigate different human blockage conditions, from low to high, in terms of blocker density, λ_b. One can deduce that 1024 RIS reflective elements are enough to surpass RIS-less transmission in the delay component for all analyzed blocker densities, λ_b.

To complement the discussion, we study the impact of the number of simultaneous transmissions on the system performance and validate our M/D/c model against computer simulations using time in the system as a parameter, as illustrated in Fig. 5. One can notice a perfect match between simulation and analytical framework for the M/D/c (multi-beam) system, which testify to the accuracy of the latter one. Recall that in the case of multi-beam operation, the power budget of an antenna has to be split among beams. To this end, we employ 1-beam and 2-beams operation for multicast system (i.e., c= $1, 2$), which is shown to be the most efficient number for the considered service area radius [19]. The behavior of the resulting curves shows the same trend with respect to the case of a single beam system.

However, we emphasize that for the multicast scenario,

TABLE I: Default Parameters.

Parameter	***Value***
Carrier frequency, f	28 GHz
Number of UEs, N_{UE}	30
Height of AP, h_A	3 m
Height of blocker, h_B	1.7 m
Height of UE, h_U	1.5 m
Blocker radius, r_B	0.4 m
Density of blockers, λ_B	0.3 bl./m^2
SNR threshold, SNR_{thr}	-9.478 dB
Transmit power, P_T	46 dBm
BS antenna array	32×32, 16×16, 8×8, 4×4, 2×2
Radius of the area of interest, R_d	100 m
SNR (MCS15, rate $948/1024$), $\text{S}_{\max}$	19.809 dB
Noise figure, NF	7.6 dB
Power spectral density of noise, N_0	174 dBm/Hz
Packet size, B	1 Gb
Number RIS elements, N_{RIS}	256 el, 1024 el
UE speed, v	0.69 m/sec

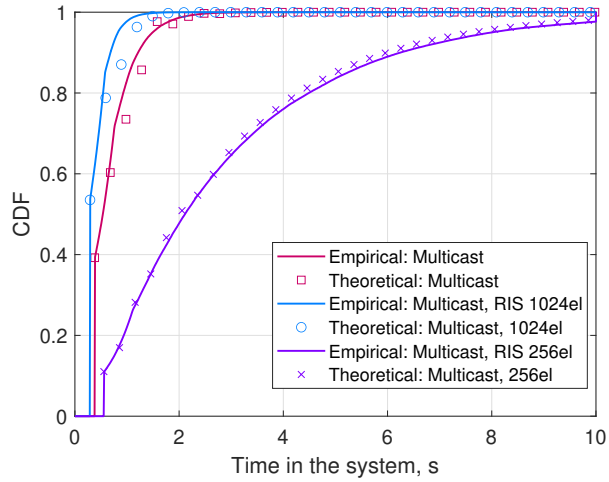

(a)

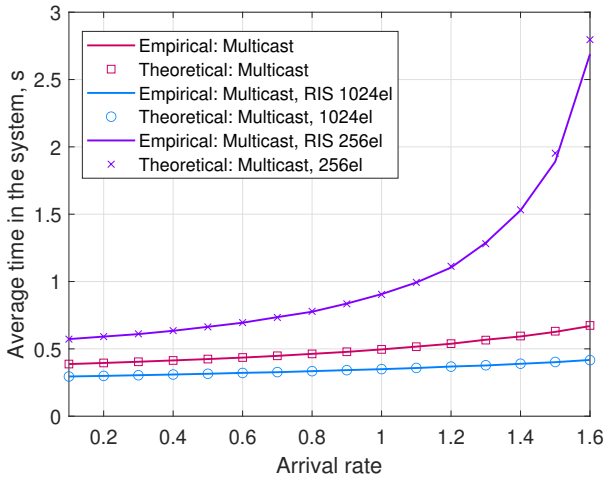

(b)

Fig. 3: Theoretical model accuracy verification for M/D/1 model, $\lambda_b = 0.7$bl./m^2: (a) CDF with arrival rate of 1.6, (b) Average time in system.

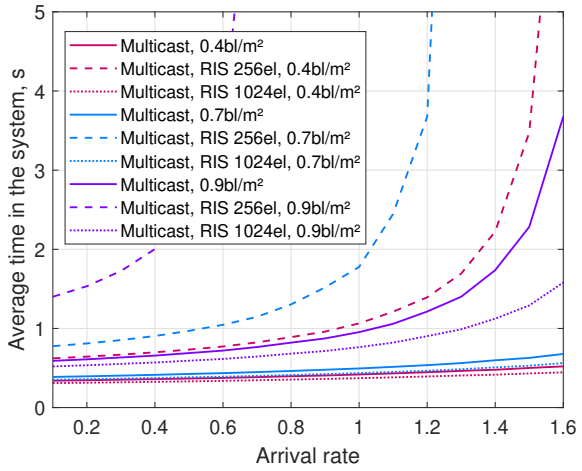

Fig. 4: Average time in system for M/D/1 model with different blocker densities, λ_b.

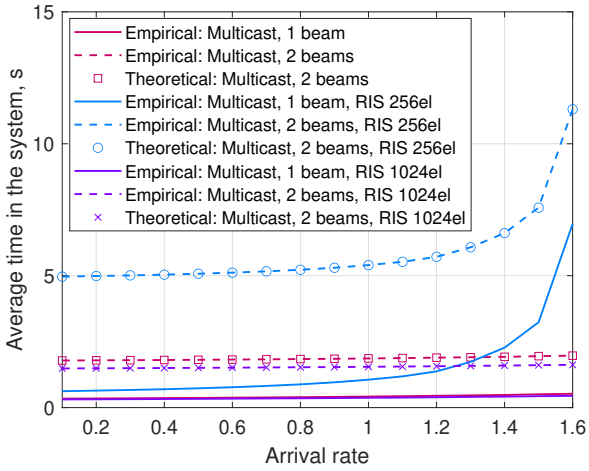

Fig. 5: Average time in system for M/D/c model with blocker density $\lambda_b = 0.4\,\text{bl/m}^2$, one-beam and multi-beam systems. Theoretical model verification for M/D/c (markers).

where users are covered with a wider beam compared to unicast, dividing the transmit power among beams might be inefficient, as proved by Fig. 5. Note that RIS-aided multicasting with 1024 reflective elements outperforms all other configurations. Differently, RIS-assisted single-beam multicasting exploiting 256 reflective elements performs poorer than the conventional multicast transmission due to the passive nature of RIS and higher transmission distances. Moreover, the performance for the system with 256 RIS elements degrades even more in the case of the 2-beams system since the transmit power has to be split among beams. However, the settings of the RIS-assisted multicast systems with a non-large antenna array could be adjusted by means of intelligent power control and allocation techniques (e.g., max-fairness power control).

As a final remark, we wish to point out that the utilized queuing model can be easily extended to multiple NR BSs and multiple RISs cases by exploiting existing UE and BS association policies.

V. Conclusions

In this work, we built a theoretical model for RIS-assisted multicast communications for future 6G wireless systems by applying the M/D/c queueing model, where c $\geq$ 1 is the number of simultaneous beams at the NR BS. Particularly, we obtained an expression of the deterministic service times for multicast and RIS-aided multicasting with single- and multi-beam antenna design based on the UEs' channel conditions.

We then validated the compact mathematical formulation via MATLAB simulator and provided a set of results when varying the blockage density and the number of beams to be utilized. We concluded that RIS with larger number of reflective elements easily excels even slightly impeded direct BS-user paths, whereas, in the case of RISs of small size, intelligent mechanisms for power control and sharing should be developed to provide better performance.

ACKNOWLEDGMENT

The authors gratefully acknowledge funding from European Union's Horizon 2020 Research and Innovation programme under the Marie Skłodowska Curie grant agreement No. 813278 (A-WEAR: A network for dynamic wearable applications with privacy constraints, http://www.a-wear.eu/).

REFERENCES

[1] E. C. Strinati, G. C. Alexandropoulos, V. Sciancalepore, M. Di Renzo, H. Wymeersch, D.-T. Phan-Huy, M. Crozzoli, R. d'Errico, E. De Carvalho, P. Popovski, *et al.*, "Wireless Environment as a Service Enabled by Reconfigurable Intelligent Surfaces: The RISE-6G Perspective," in *2021 Joint European Conference on Networks and Communications & 6G Summit (EuCNC/6G Summit)*, pp. 562–567, IEEE, 2021.

[2] N. Chukhno, O. Chukhno, S. Pizzi, A. Molinaro, A. Iera, and G. Araniti, "Efficient Management of Multicast Traffic in Directional mmWave Networks," *IEEE Transactions on Broadcasting*, vol. 67, no. 3, pp. 593–605, 2021.

[3] G. Zhou, C. Pan, H. Ren, K. Wang, and A. Nallanathan, "Intelligent Reflecting Surface Aided Multigroup Multicast MISO Communication Systems," *IEEE Transactions on Signal Processing*, vol. 68, pp. 3236–3251, 2020.

[4] C. Pan, H. Ren, K. Wang, J. F. Kolb, M. Elkashlan, M. Chen, M. Di Renzo, Y. Hao, J. Wang, A. L. Swindlehurst, *et al.*, "Reconfigurable Intelligent Surfaces for 6G systems: Principles, Applications, and Research Directions," *IEEE Communications Magazine*, vol. 59, no. 6, pp. 14–20, 2021.

[5] L. Du, S. Shao, G. Yang, J. Ma, Q. Liang, and Y. Tang, "Capacity Characterization for Reconfigurable Intelligent Surfaces Assisted Multiple-Antenna Multicast," *IEEE Transactions on Wireless Communications*, vol. 20, no. 10, pp. 6940–6953, 2021.

[6] B. Sihlbom, M. I. Poulakis, and M. Di Renzo, "Reconfigurable Intelligent Surfaces: Performance Assessment Through a System-Level Simulator," *arXiv preprint arXiv:2111.10791*, 2021.

[7] I. Yildirim, A. Uyrus, and E. Basar, "Modeling and Analysis of Reconfigurable Intelligent Surfaces for Indoor and Outdoor Applications in Future Wireless Networks," *IEEE Transactions on Communications*, vol. 69, no. 2, pp. 1290–1301, 2020.

[8] E. Basar, I. Yildirim, and F. Kilinc, "Indoor and Outdoor Physical Channel Modeling and Efficient Positioning for Reconfigurable Intelligent Surfaces in mmWave Bands," *IEEE Transactions on Communications*, vol. 69, no. 12, pp. 8600–8611, 2021.

[9] F. Farina, D. Fontanelli, A. Garulli, A. Giannitrapani, and D. Prattichizzo, "Walking Ahead: The Headed Social Force Model," *PloS one*, vol. 12, no. 1, p. e0169734, 2017.

[10] O. Chukhno, N. Chukhno, O. Galinina, Y. Gaidamaka, S. Andreev, and K. Samouylov, "Analysis of 3D Deafness Effects in Highly Directional mmWave Communications," in *2019 IEEE Global Communications Conference (GLOBECOM)*, pp. 1–6, IEEE, 2019.

[11] 3GPP, "Study on Channel Model for Frequencies from 0.5 to 100 GHz (Release 16)," 3GPP TR 38.901 V16.1.0, November 2020.

[12] S. W. Ellingson, "Path loss in Reconfigurable Intelligent Surface-enabled Channels," in *2021 IEEE 32nd Annual International Symposium on Personal, Indoor and Mobile Radio Communications (PIMRC)*, pp. 829–835, IEEE, 2021.

[13] J. G. Andrews, T. Bai, M. N. Kulkarni, A. Alkhateeb, A. K. Gupta, and R. W. Heath, "Modeling and Analyzing Millimeter Wave Cellular Systems," *IEEE Transactions on Communications*, vol. 65, no. 1, pp. 403–430, 2016.

[14] G. R. MacCartney, T. S. Rappaport, and S. Rangan, "Rapid Fading Due to Human Blockage in Pedestrian Crowds at 5G Millimeter-Wave Frequencies," in *GLOBECOM 2017-2017 IEEE Global Communications Conference*, pp. 1–7, IEEE, 2017.

[15] M. Gapeyenko, A. Samuylov, M. Gerasimenko, D. Moltchanov, S. Singh, E. Aryafar, S.-p. Yeh, N. Himayat, S. Andreev, and Y. Koucheryavy, "Analysis of Human-Body Blockage in Urban Millimeter-Wave Cellular Communications," in *2016 IEEE International Conference on Communications (ICC)*, pp. 1–7, IEEE, 2016.

[16] A. K. Erlang, "The Theory of Probabilities and Telephone Conversations," *Nyt. Tidsskr. Mat. Ser. B*, vol. 20, pp. 33–39, 1909.

[17] G. J. Franx, "A Simple Solution for the M/D/c Waiting Time Distribution," *Operations Research Letters*, vol. 29, no. 5, pp. 221–229, 2001.

[18] F. Chiariotti, O. Vikhrova, B. Soret, and P. Popovski, "Peak Age of Information Distribution for Edge Computing with Wireless Links," *IEEE Transactions on Communications*, vol. 69, no. 5, pp. 3176–3191, 2021.

[19] N. Chukhno, O. Chukhno, D. Moltchanov, A. Molinaro, Y. Gaidamaka, K. Samouylov, Y. Koucheryavy, and G. Araniti, "Optimal Multicasting in Millimeter Wave 5G NR with Multi-beam Directional Antennas," *IEEE Transactions on Mobile Computing (Early Access)*, 2021.